Science Signaling
AAAS

www.sciencesignaling.org/cgi/content/full/11/536/eaao2387/DC1

Supplementary Materials for

MEG3-4 is a miRNA decoy that regulates IL-1β abundance to initiate and then limit inflammation to prevent sepsis during lung infection

Rongpeng Li, Lizhu Fang, Qinqin Pu, Huimin Bu, Pengcheng Zhu, Zihan Chen, Min Yu, Xuefeng Li, Timothy Weiland, Arvind Bansal, Shui Qing Ye, Yuquan Wei, Jianxin Jiang,* Min Wu*

*Corresponding author. Email: min.wu@med.und.edu (M.W.); hellojjx@126.com (J.J.)

Published 26 June 2018, *Sci. Signal.* **11**, eaao2387 (2018)
DOI: 10.1126/scisignal.aao2387

This PDF file includes:

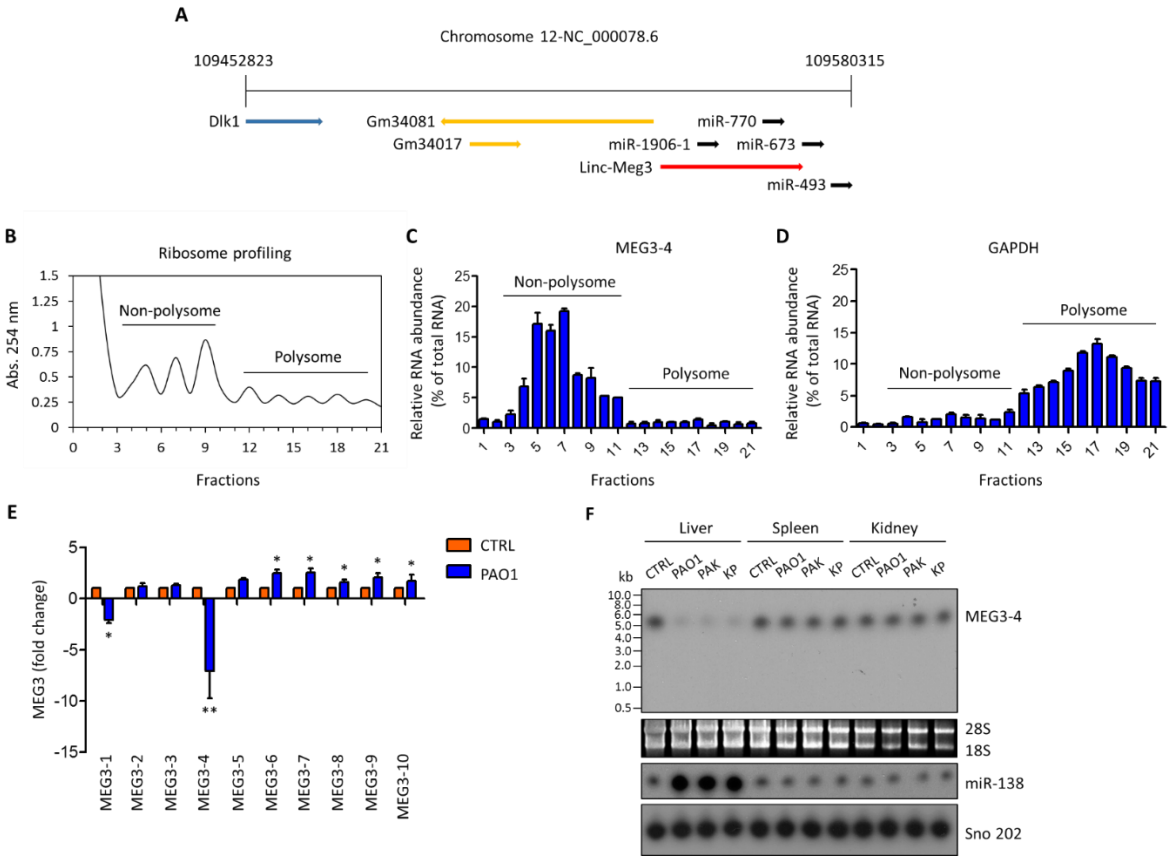

Figure S1. Characterization of lncRNA MEG3. (A) Schematic of the gene *Meg3* located in chromosome 12, without overlapping with protein coding genes but overlapping with miR-1906-1 and miR-770. One protein-coding gene [*Delta-like 1 homolog* (*Dlk1*)], two predicted genes (*Gm34081* and *Gm34017*), and two miRNAs (miR-493 and miR-673) neighbor *Meg3*. **(B)** The polyribosome and non-polyribosome fractions, as shown by the profile of the absorbance at 254 nm, were separated by sucrose gradient centrifugation of mouse lung homogenates. Data are representative of n=3 mice. **(C)** The abundance of MEG3-4 transcripts in the polyribosome and non-polyribosome fractions as measured by qPCR and normalized to total MEG3 in all the fractions. **(D)** The abundance of *Gapdh* transcripts in the polyribosome and non-polyribosome fractions as measured by qPCR normalized to total *Gapdh* in all the fractions. **(E)** C57BL/6J mice (n = 3) were intranasally infected with 5×10^6 colony forming units (CFU) of PAO1 per mouse for 24 hours. qPCR analysis of individual MEG3 transcript expression in PAO1-infected mouse lungs. CTRL: control. **(F)** Northern blotting analysis of MEG3-4 and miR-138 expression in mouse livers, spleens, and kidneys after PAO1, PAK, or KP infection. Detection of 18S and 28S rRNA and Sno202 snRNA was used as loading controls for MEG3-4 and miR-138, respectively. Data in (**B**) and (**F**) are representative of n=3 mice. Data in (**C-E**) are means ± SD for three independent mouse lungs. $*P \leq 0.05$, $**P \leq 0.01$ by Kruskal-Wallis test.

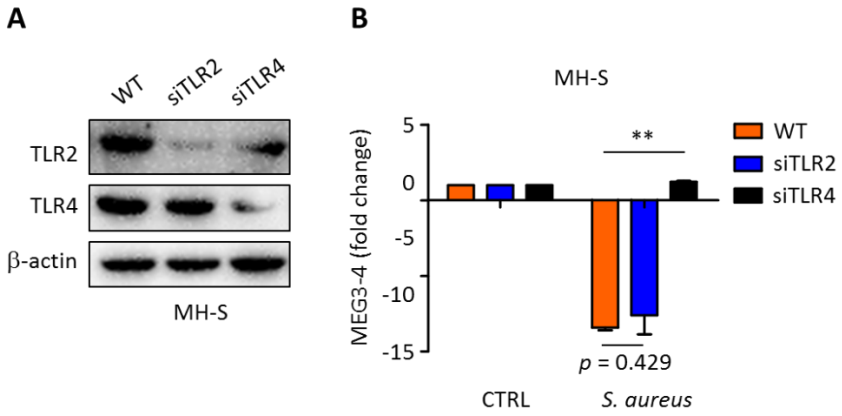

Figure S2. MEG3-4 inhibition signaling in alveolar macrophage cells is TLR4-specific during *S. aureus* infection. (A) Murine alveolar macrophage MH-S cells were transfected with control siRNA (siNC), TLR2 siRNA (siTLR2) or TLR4 siRNA (siTLR4) for 48 hours, then TLR2 and TLR4 abundance was measured by immunoblotting (representative of n=3 experiments). **(B)** Change in MEG3-4 abundance in siNC-, siTLR2- or siTLR4-transfected MH-S cells infected with *S. aureus* at 20:1 MOI for 2 hours relative to controls (CTRL). Data are mean ± SD of n=3 experiments. $^{**}P \leq 0.01$ by Kruskal-Wallis test.

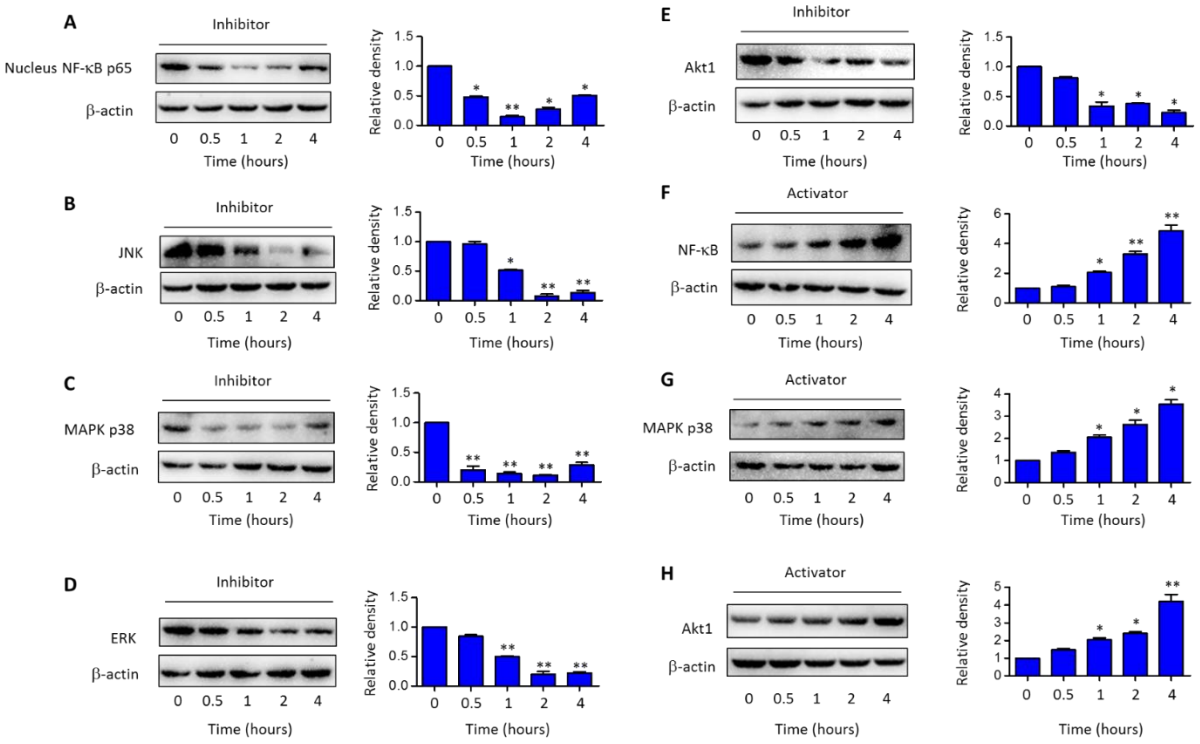

Figure S3. Immunoblotting validation of signaling factors in inhibitor- or activator-treated MH-S cells. (A-H) Immunoblotting assessment of the abundance of select proteins after MH-S cells were treated with the indicated signaling pathway activators or inhibitors: NF-κB inhibitor SN50 (**A**), JNK inhibitor SP600125 (**B**), p38 inhibitor SB203580 (**C**), ERK inhibitor FR180204 (**D**), AKT inhibitor GSK690693 (**E**), NF-κB activator betulinic acid (**F**), JNK/p38 activator anisomycin (**G**), and AKT activator SC79 (**H**), each at 10 nM for 4 hours. Blots are representative and data are means ± SD of three independent cell samples. *$P \leq 0.05$, **$P \leq 0.01$ by Kruskal-Wallis test.

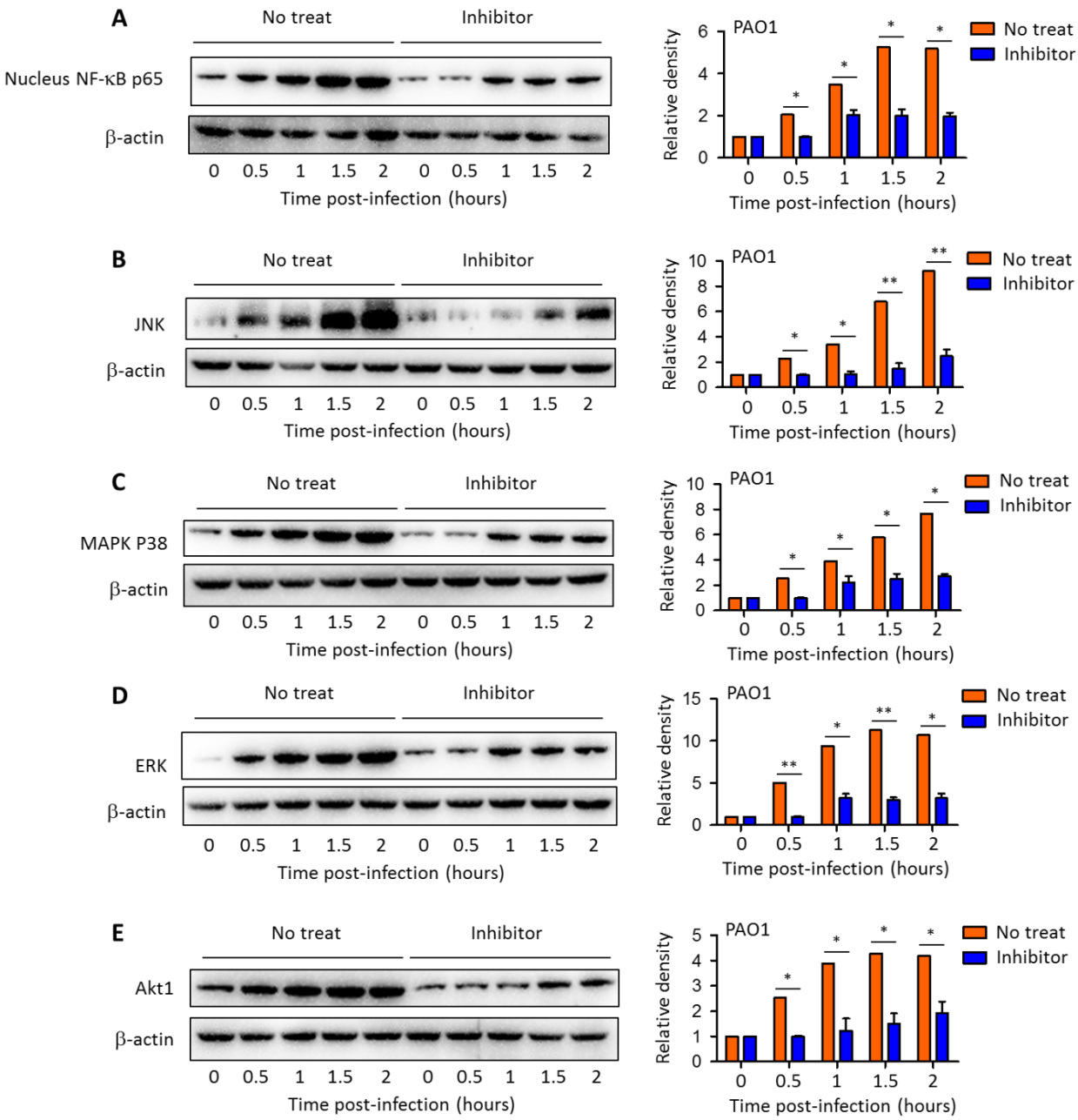

Figure S4. Dissection of signaling molecules in PAO1-infected MH-S cells. (A-E) Immunoblotting assessment of the abundance of select proteins in MH-S cells that were pretreated for 4 hours with the indicated signaling pathway inhibitor (as described in fig. S3) and then infected with PAO1 (for 2 hours at MOI of 20:1). Blots are representative and data are means ± SD of three independent cell samples. ; *$P \leq 0.05$, **$P \leq 0.01$ by Kruskal-Wallis test.

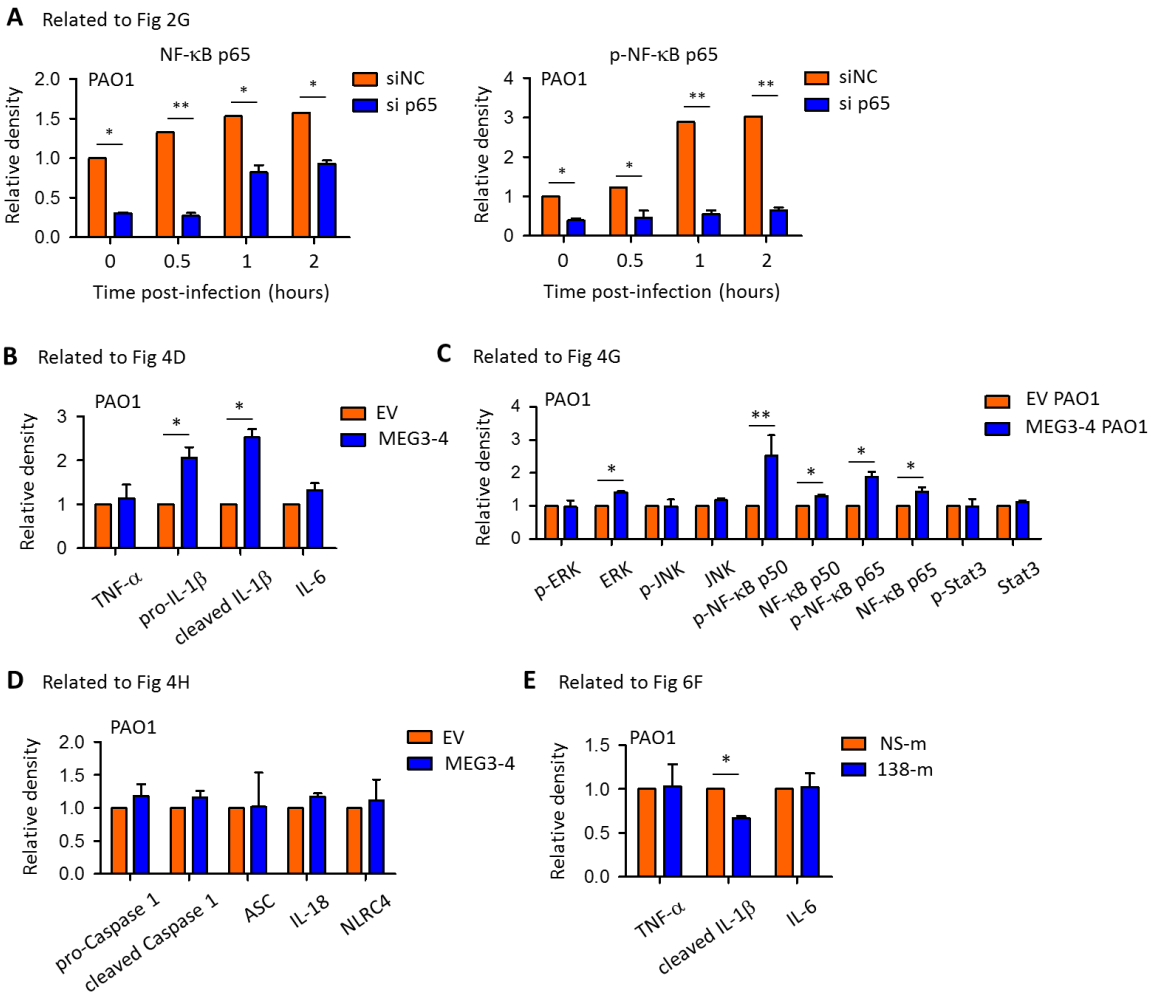

Figure S5. Densitometric quantification of the immunoblotting data. (A-E) Densitometric analysis of the immunoblots represented in, Fig. 2G (**A**), Fig. 4D (**B**), Fig. 4G (**C**), Fig. 4H (**D**), and Fig. 6F (**E**) using Quantity One software. Data are means ± SD of three reproducible gels. **P* ≤ 0.05, ***P* ≤ 0.01 by Kruskal-Wallis test. siNC: nonspecific control siRNA; si p65: NF-κB p65 siRNA; EV: empty vector; NS-m: nonspecific control mimics; 138-m: miR-138 mimics.

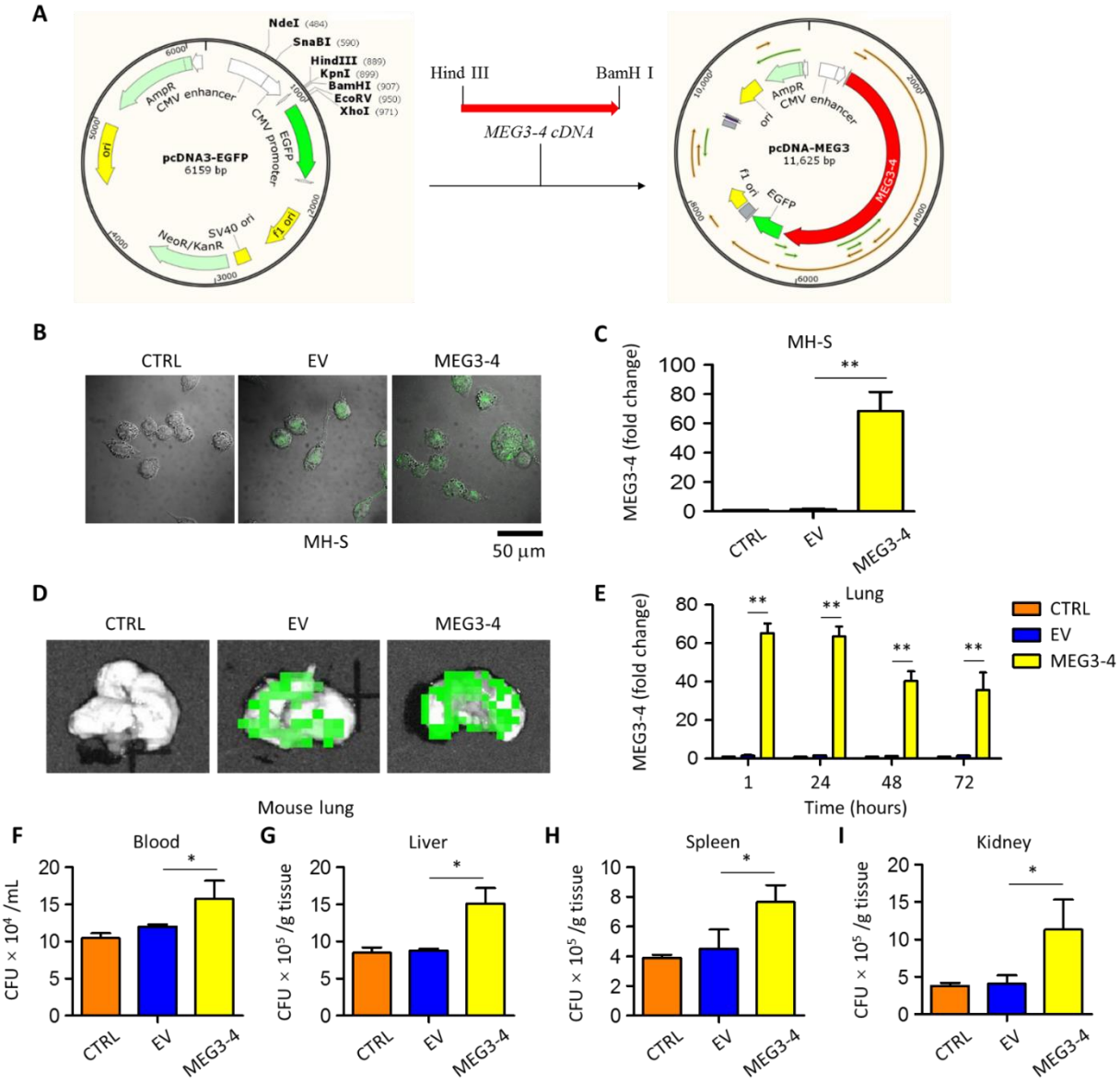

Figure S6. Restoration of the phenotype in a MEG3-4–overexpressing model. (A) Diagram of pcDNA3.1-MEG3-4 (pWT-MEG3) construction. **(B)** Confocal microscopy of MH-S cells stably transfected with pWT-MEG3 or empty vector (EV; pcDNA3-EGFP). Successful plasmid expression in MH-S cells was confirmed by the enhanced green fluorescent protein (EGFP) marker. CTRL: control, untransfected cells. Scale bar: 50 µm. **(C)** qRT-PCR analyzed MEG3-4 expression in pWT-MEG3–transfected MH-S cells. **(D)** IVIS XRII in vivo imaging of lungs from C57BL/6J mice 72 hours after intranasal infusion with pWT-MEG3–transfected MH-S cells (5×10^6 cells for each MEG3-4 mouse). EGFP signal marks pWT-MEG3 expression. Images are representative of n = 3 mice. **(E)** qRT-PCR analysis of MEG3-4 expression in lungs from mice described in (**D**). **(F-I)** Bacterial burdens in the blood, liver, spleen and kidneys of mice described in (**D**) and infected with PAO1 for 24 hours. Data in (**B**) and (**D**) are representative of three independent experiments (cell samples or mice). Data in (C and F-I) are means ± SD of three independent experiments (cell samples or mice). $*P \leq 0.05$, $**P \leq 0.01$ by Kruskal-Wallis test.

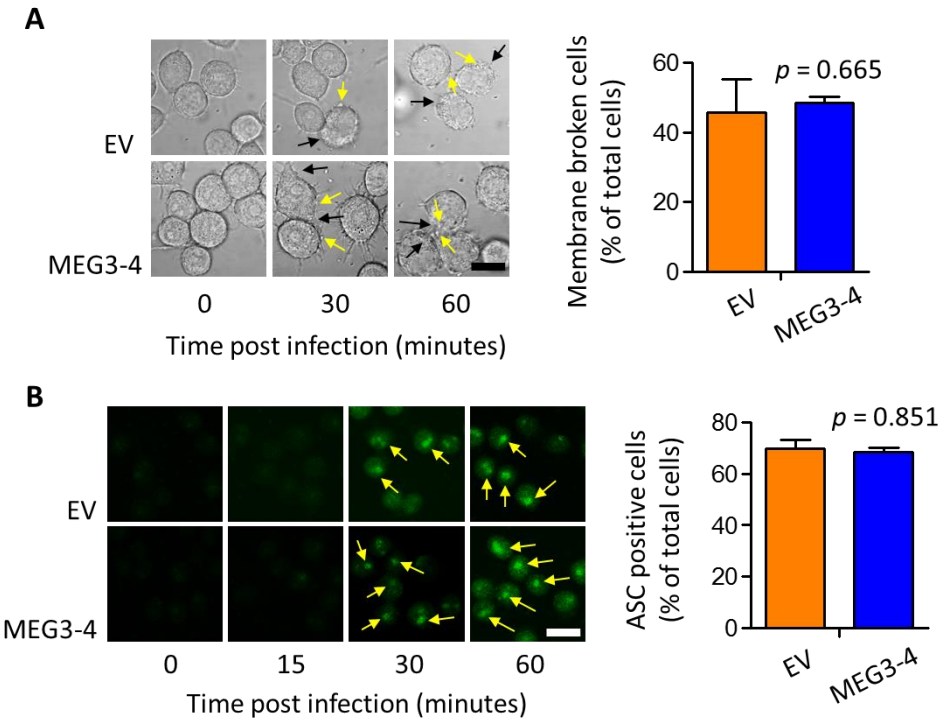

Figure S7. Imaging of pyroptosis in MH-S cells. (A) Confocal microscopy of plasma membrane rupture (black arrows) and membrane vesicles (yellow arrows) in empty vector (EV; pcDNA3-EGFP)- or MEG3-4–transfected MH-S cells that were infected with PAO1 (at an MOI of 20:1 for 0-60 minutes). Scale bar: 20 μm. **(B)** Confocal laser scanning microscopy (CSLM) the production of ASC (yellow arrows) in MH-S cells described in (**A**). Scale bar, 20 μm. Graphs, right: Images are representative and data are means ± SD of random 100 cells in three independent cell samples. Data were analyzed by Kruskal-Wallis test.

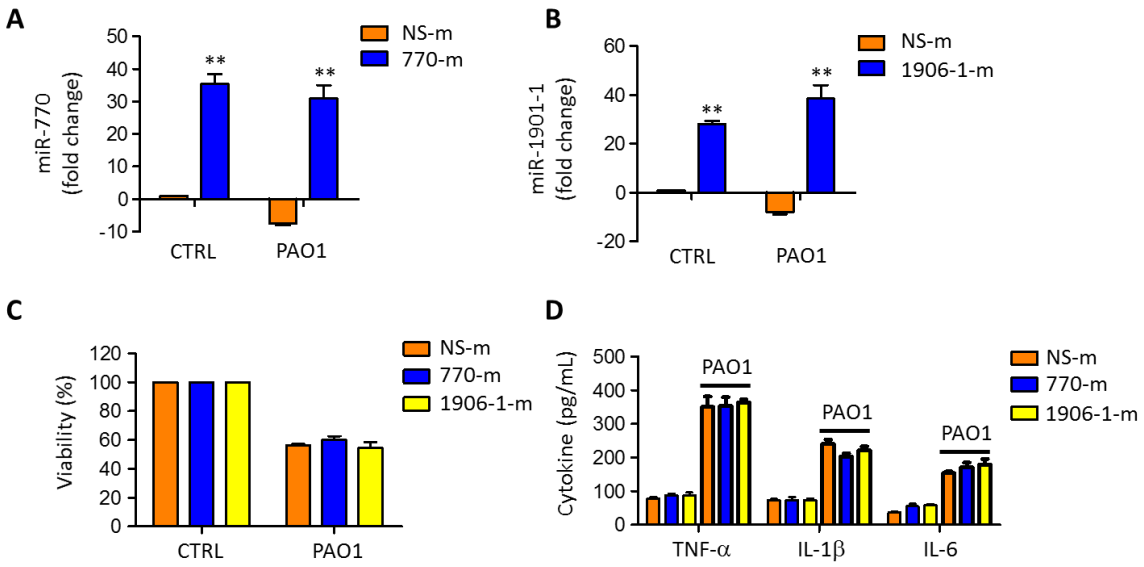

Figure S8. Functional analysis of miRNAs generated by MEG3-4. (A-B) qRT-PCR analysis of miR-770 and miR-1906-1 expression in MH-S cells transfected with nonspecific mimics (NS-m), miR-770 mimics (770-m), or miR-1906-1 mimics (1906-1-m; 50 ng) for 24 hours then infected with PAO1 (at an MOI of 20:1) for 2 hours. **(C)** Viability of the cells described in (**A-B**) as determined by MTT assay at a wavelength of 570 nm. **(D)** Abundance of inflammatory cytokines in the cells described in (A-B) as assessed by ELISA. Data are means ± SD of three independent cell samples. $^{**}P \leq 0.01$ by Kruskal-Wallis test.

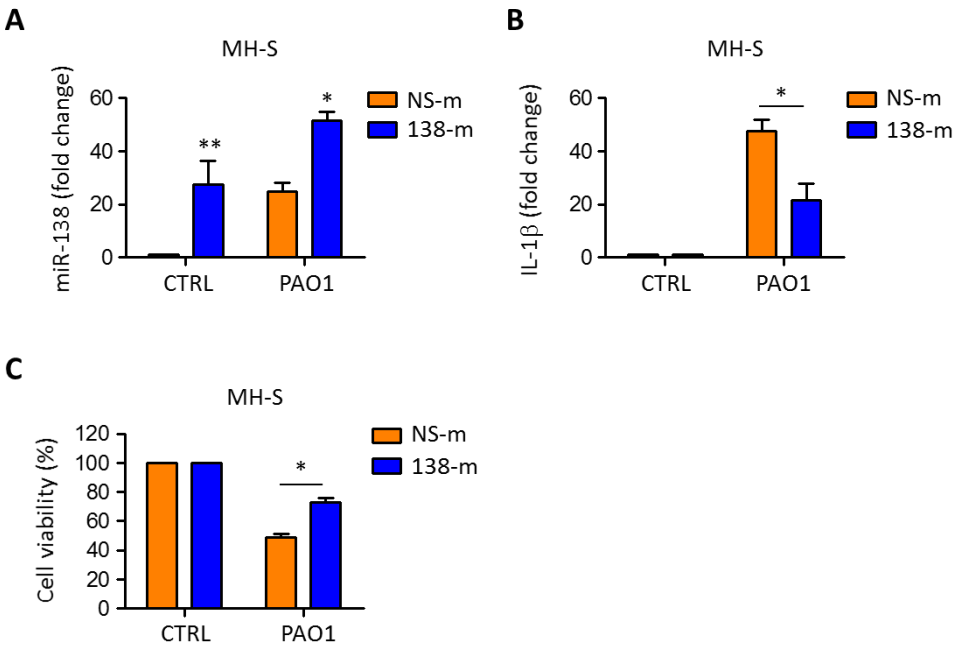

Figure S9. miR-138 regulates IL-1β expression and cell viability in alveolar macrophages. **(A-B)** qRT-PCR analysis of the abundance of miR-138 (**A**) and IL-1β–encoding mRNA (**B**) in MH-S cells that were transfected with nonspecific control mimics (NS-m) or miR-138 mimics (138-m; 50 ng) for 24 hours and then infected with PAO1 (at an MOI of 20:1) for 30 minutes. **(C)** Viability of the cells described in (**A** and **B**) were measured by MTT assay. Data are means ± SD of three independent cell samples. *$P \leq 0.05$, **$P \leq 0.01$ by Kruskal-Wallis test.

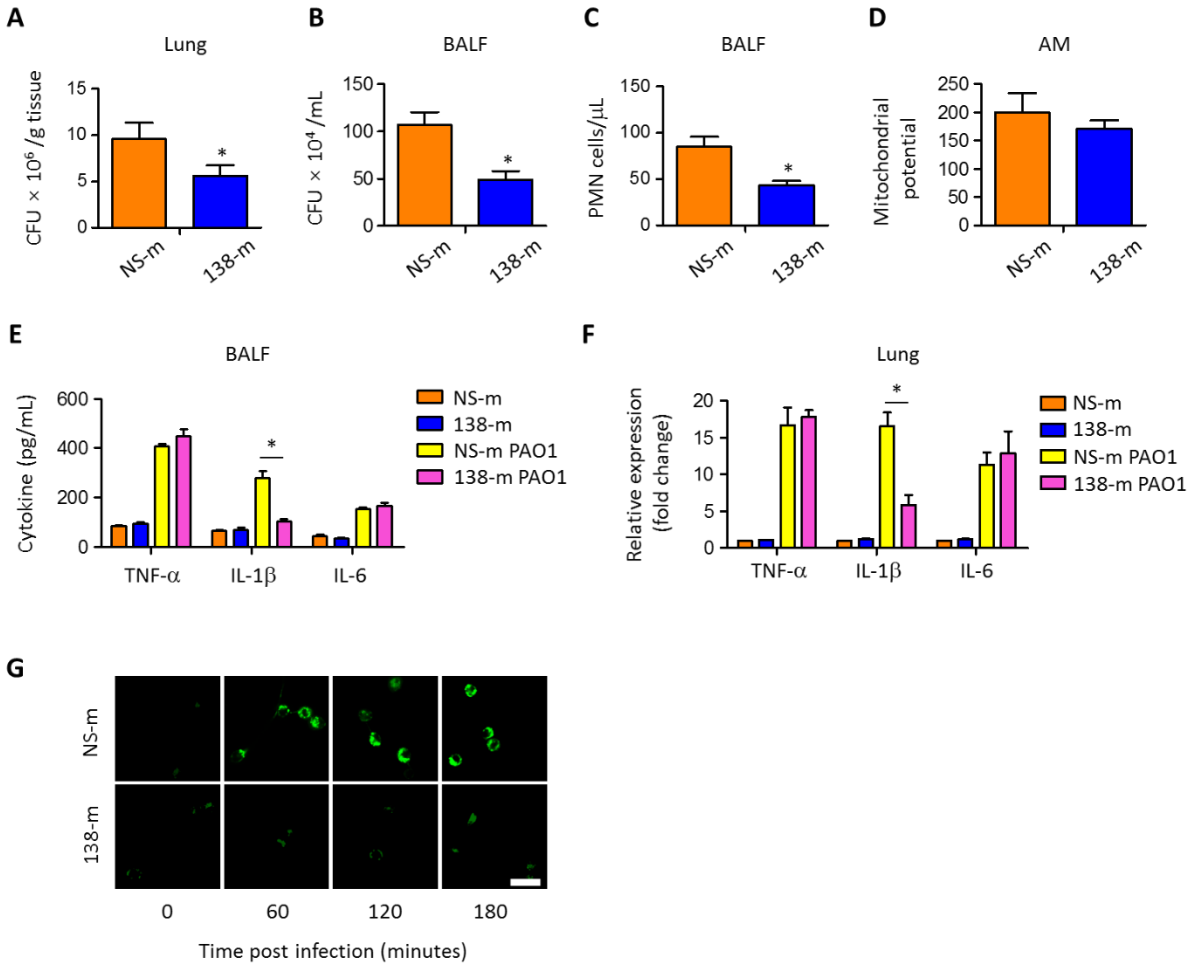

Figure S10. miR-138 enhances host defense against *P. aeruginosa* by repressing IL-1β expression in mouse lungs. (A-B) Bacterial burden in the lungs and bronchoalveolar lavage fluid (BALF) from mice first i.v. injected with miR-138 mimics (138-m) or a nonspecific control mimic (NS-m) then intranasally infected with 5×10^6 CFU of PAO1) for 24 hours was determined by plating samples on agar dishes. **(C)** PMN cell percentage relative to total nuclear cells was evaluated in BALF from mice described in (**A-B**), assessed by HEMA-3 staining. **(D)** Mitochondrial potential of alveolar macrophages measured by JC-1 fluorescence assay. **(E)** Cytokine levels in BALF from mice described in (**A-B**) as assessed by ELISA. **(F)** Expression of cytokines in the lungs from mice described in (**A-B**) as assessed by qRT-PCR. **(G)** Alveolar macrophages were isolated from wild-type mouse lungs and transfected in culture with NS-m or miR-138 mimics (50 ng) for 24 hours then challenged with PAO1 (at an MOI of 20:1) for 0-120 min. Confocal laser scanning microscopy (CSLM) then assessed the abundance of IL-1β immunochemistry in those alveolar macrophages. Scale bar, 50 μm. Data are means ± SD from three mice. *$P \leq 0.05$ by Kruskal-Wallis test. Data in (**G**) are representative of cells isolated from three mice.

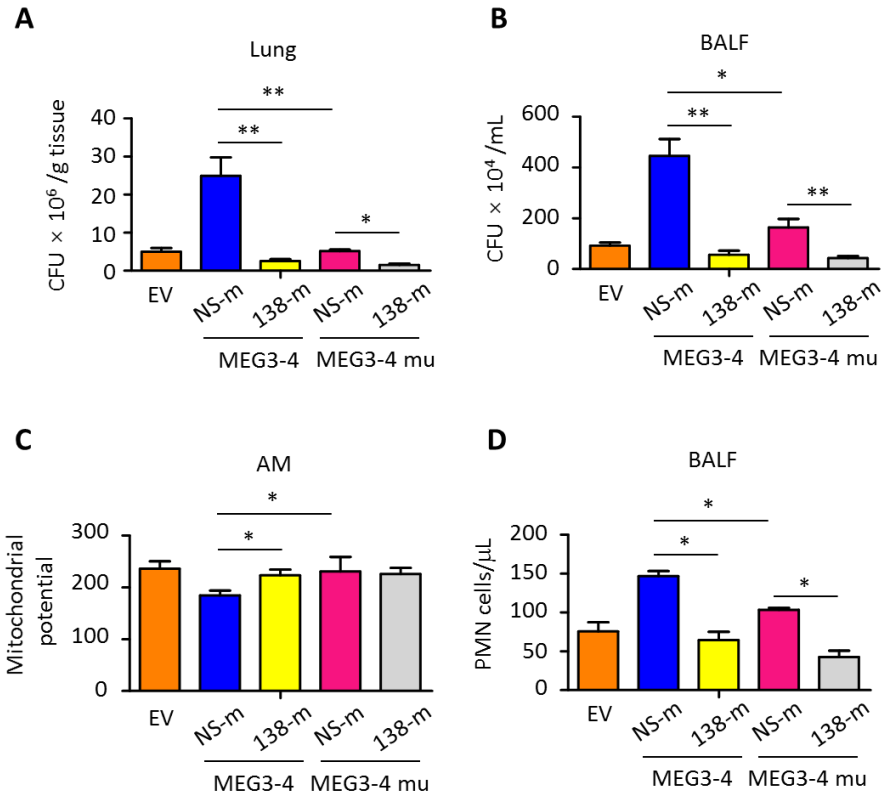

Figure S11. **MEG3-4 overexpression phenotypes in mice were reversed by treatment with 138-m. (A-B)** Bacterial burdens in the lungs and BALF from mice that were intranasally instilled with either stable MH-S cells expressing wild-type or mutant (mu) MEG3-4 and then were intravenously injected with vehicle containing either nonspecific control mimics (NS-m) or miR-138 mimics (138-m; 50 μg per mouse) for 24 or 48 hours before PAO1 challenge (at 5×10^6 CFU) for 24 hours (n=3 mice per condition). **(C)** PMN percentages relative to total nuclear cells in BALF isolated from mice described in (**A-B**), measured with HEMA-3 staining. **(D)** Mitochondrial potential of alveolar macrophages isolated from mice described in (A-B), measured by JC-1 fluorescence assay. Data are means ± SD of three mice. $*P \leq 0.05$, $**P \leq 0.01$ by Kruskal-Wallis test.

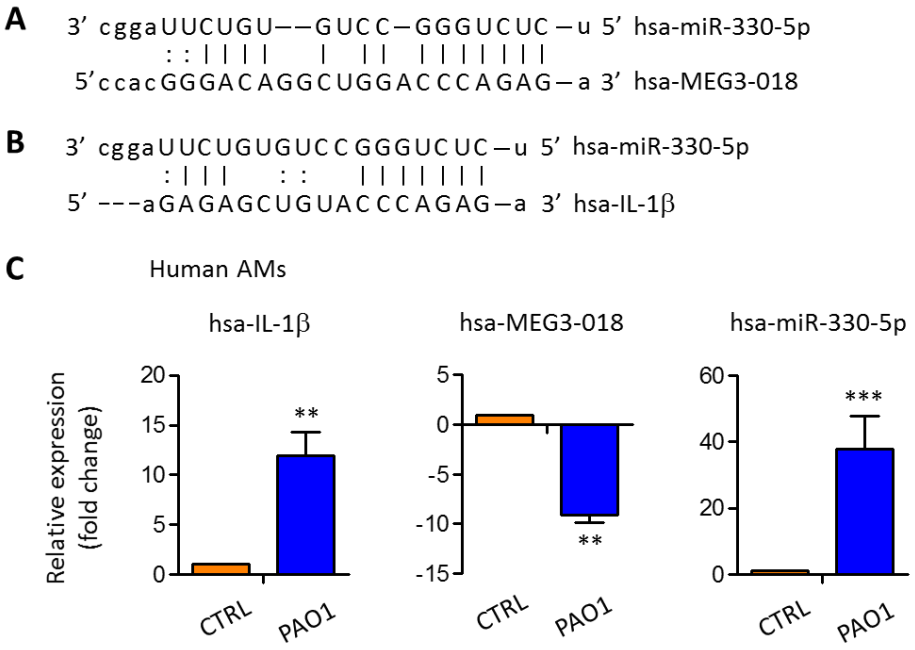

Figure S12. Analysis of MEG3 function and expression in human alveolar macrophages. **(A)** Duplex formations between human MEG3 transcript 18 (bottom) and miR-330-5p (top). **(B)** 3'UTRs in mRNA encoding human IL-1β (bottom) contain predicted binding sequences for miR-330-5p (top). **(C)** Primary human alveolar macrophages were infected with PAO1 (at an MOI of 20:1) for 2 hours, then expression of has-MEG3-18, has-miR-330-5p and has-*IL1B* mRNA was assessed by qRT-PCR. Data are means ± SD for three independent cell samples. $^{**}P \leq 0.01$, $^{***}P \leq 0.001$ by Kruskal-Wallis test.

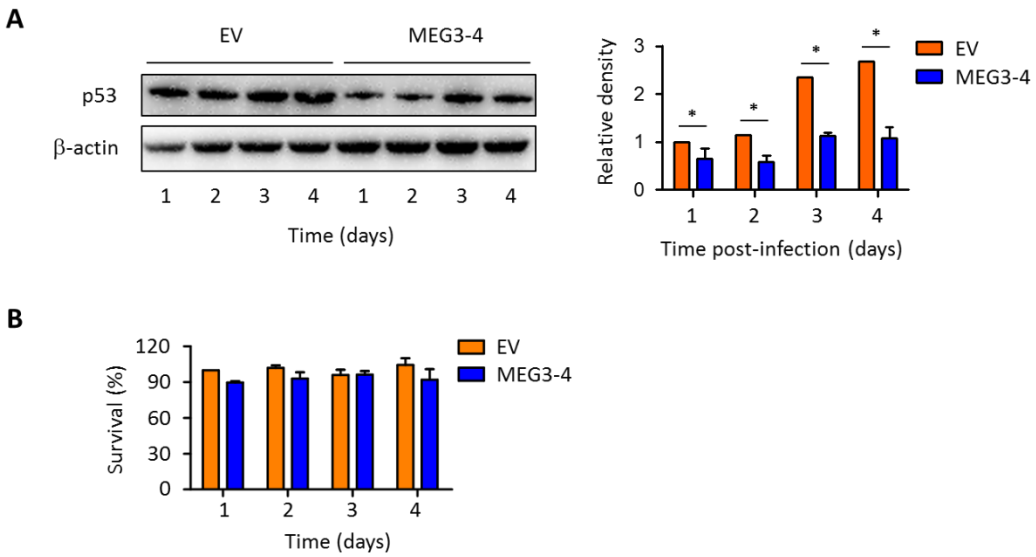

Figure S13. MEG3-4 overexpression inhibits p53 expression in mouse B16 melanoma tumor cells. (A) Immunoblotting for p53 in B16 cells assessed over 4 days in selection culture after a 24-hour transfection with pWT-MEG3 or empty vector (EV; pcDNA3-EGFP). **(B)** Viability of cells described in (**A**) as determined by MTT assay. Blot is representative and data are means ± SD of three independent cell samples. *$P \leq 0.05$ by Kruskal-Wallis test.

Table S1. lncRNA expression in response to PAO1 infection. Fold changes of regulated lncRNAs upon PAO1 infection in mouse lungs. Red highlights MEG3-4 analysis. Data are related to those shown in Figure 1.

Gene symbol	Fold Change (PAO1 vs CTRL)	Gene symbol	Fold Change (PAO1 vs CTRL)
1500012K07Rik	65.0274	*D930015M05Rik*	10.7061
1810019N24Rik	18.7371	*Dleu2*	3.1575
1810058I24Rik	2.3404	*Dlx1as*	44.5694
2010300F17Rik	20.6535	*Firre*	2.2416
2210406O10Rik	20.909	*Gas5*	4.3984
2310001H17Rik	4.4284	*Gm12116*	43.7018
2500004C02Rik	13.5866	*Gm13111*	4.3528
2900041M22Rik	30.5471	*Gm14204*	135.1969
4921504A21Rik	23.5417	*Gm14379*	62.5014
4930470G03Rik	45.8176	*Gm14705*	3.3951
4930554H23Rik	47.6624	*Gm15050*	5.1656
4930555B11Rik	68.0011	*Gm15832*	21.9342
4930558J18Rik	84.0461	*Gm16023*	11.3067
4931440J10Rik	86.0052	*Gm16575*	9.4167
4932412D23Rik	65.4387	*Gm16754*	7.8118
4933407K13Rik	10.1736	*Gm16892*	15.0422
4933427G23Rik	47.6867	*Gm16933*	65.6773
5530601H04Rik	6.4103	*Gm16998*	51.0418
5730480H06Rik	6.1394	*Gm17275*	4.2265
5830418P13Rik	38.8651	*Gm17337*	44.3548
5830432E09Rik	11.8134	*Gm17354*	8.5083
6820431F20Rik	5.7193	*Gm17388*	2.4207
9330158H04Rik	3.4425	*Gm17473*	13.2815
9430037G07Rik	13.0248	*Gm4117*	32.1516
9530052C20Rik	6.9593	*Gm4211*	51.8984
9530059O14Rik	31.1323	*Gm5602*	25.785
9630001P10Rik	3.4786	*Gm6410*	16.8958
A230107N01Rik	41.8523	*Gm6999*	56.7762
A330023F24Rik	4.2369	*Hotair*	103.1528
A430010J10Rik	135.3532	*Jpx*	12.6558
A430108G06Rik	19.9442	*Pcsk2os1*	100.4333
A930024N18Rik	18.2943	*Redrum*	77.4611
Atxn7l1os2	28.8071	*Rmst*	100.7064
C130071C03Rik	13.8662	*Zfa-ps*	47.4371
C330013F16Rik	9.6621	*Snora73b*	3.5776
Ccdc41os1	14.1056	*C130021I20Rik*	-2.6038
Chd3os	6.6091	***Meg3***	**-18.1744**
D430036J16Rik	5.2575	*Rplp0*	-4.6374

Table S2. Primers used in this study. Sequences of the primers used in this study. F, forward; R, reverse; Mu, mutant.

Name	Sequence (5' to 3')
For plasmid construction	
pcDNA3-EGFP	
MEG3-4 F	CCC**AAGCTT**AGAATAAGTGGGGACAATG (Hind III)
MEG3-4 R	CG**GGATCC**CCATTCTCCTTCCCCTTAAG (BamH I)
pMD19-T	
138 F	CAGGAAAAGTCTGCTATAGGAG
138 R	GGATGCTTGTTGCTTGCTGCTC
pGL3	
MEG3-4 F	GC**TCTAGA**GTAGCTCTTGGGTGTGTC (Xba I)
MEG3-4 R	AA**GGCCGGCC**TCCATTCTCCTTCCCCTTAAG (Fse I)
MEG3-4 Mu1	TGAGATAGCTAAATATCTTTCAGGCTCAGGTGTTGATA
MEG3-4 Mu2	TATCAACACCTGAGCCTGAAAGATATTTAGCTATCTCA
IL1B F	GC**TCTAGA**AGTATGGGCTGGACTG (Xba I)
IL1B R	AA**GGCCGGCC**GTTTTAATGAAATTTATTTC (Fse I)
IL1B Mu1	TGGATGAGACTTTTACAGACGGGGTGTTAATACATTGCTTT
IL1B Mu2	AAAGCAATGTATTAACACCCCGTCTGTAAAAGTCTCATCCA
For quantitative real-time PCR	
MEG3-1 F	GCACATGGAGACTGGAGCTA
MEG3-1 R	TCAGGACAGGGAGTTGTGAG
MEG3-2 F	TAAATGAACTGCAGCAGCCT
MEG3-2 R	GCGAGAGAATGGTTGAGACA
MEG3-3 F	CATCTGTGAAATGGGCTCAG
MEG3-3 R	GAAAGCACCATGAGCCACTA
MEG3-4 F	GGGACCATGGGTTCATTTAC
MEG3-4 R	CACCCTAAATCACACAGCCA
MEG3-5 F	TGAACCAGTGCCCTAGTGAG
MEG3-5 R	GGAAAGGGCTCAGACTCAAG
MEG3-6 F	GGAAAGGGCTCAGACTCAAG
MEG3-6 R	AGGTGGGTCTCTCTACTCAAGG
MEG3-7 F	CTTGAGTCTGAGCCCTTTCC
MEG3-7 R	GGCAGCACTCCAGTTCACTA
MEG3-8 F	GAGGACTCCACCCACGAC
MEG3-8 R	GAGGACTCCACCCACGAC
MEG3-9 F	CTCGAAATCCTAGCCATCGT
MEG3-9 R	CCATGGACTCTCAAGGACAA
MEG3-10 F	CCATGGACTCTCAAGGACAA
MEG3-10 R	CCATGGACTCTCAAGGACAA
GAPDH F	ACAACTTTGGCATTGTGGAA
GAPDH R	GATGCAGGGATGATGTTCTG
IL1B F	CCAAAGAAGAGGGACAAAGG

IL1B R	TGCTGGTGCTTCTTCTGTCT
TNFa F	GCCAACAACACCAGAAACAC
TNFa R	CTGGTCTTTCCGCCTCTTC
IL6 F	CCACGAAGAACGACAAAGAA
IL6 R	GGTCTTTCTTCCGCCTCTG
ERK1 F	TGCGACCTTAAGATCTGTGATT
ERK1 R	AGTGTGGTCGTGCTCAGG
ERK2 F	TGAAGTTGAACAGGCTCTGG
ERK2 R	AGTCGTCCAACTCCATGTCA
JNK1 F	TCAAGCACCTTCACTCTGCT
JNK1 R	AGTCACCACATAAGGCGTCA
JNK2 F	GTGATTGATCCAGACAAGCG
JNK2 R	TTCCAACTGGGCATCATAAA
P50 F	CCTCTCTCGTCTTCCTCCAC
P50 R	CCTCTCTCGTCTTCCTCCAC
P65 F	CTCACCGGCCTCATCCACAT
P65 R	TTGGTCTGGATTCGCTGGCT
Stat3 F	TCGTGGAGCTGTTCAGAAAC
Stat3 R	GGAAATTTGACCAGCAACCT
miR-129-5p	CTTTTTGCGGTCTGGGCTTGC
miR-136	TAATGCCCCTAAAAATCCTTAT
miR-138	AGCTGGTGTTGTGAATAGGCCG
miR-770	AGCACCACGTGTCTGGGCCACG
miR-1906-1	TGCAGCAGCCTGAGGCAGGGCT
Sno202	GTTGGCTCTGGTGCAGGGTCCGAGGTAT
For Northern blotting and ISH	
MEG3 general	GTCCTCAGTCTTCTTTTCTTCAGCCGGCATGG
MEG3-4 special	GCTTGGGGGGGGGGGGCAGAGCCCACATCA
miR-138	CGGCCTGATTCACAACACCAGCT
Sno202	ATACCTCGGACCCTGCACCAGAGCCAAC
For CLIP and LAMP assay	
MEG3-4 F	GAGAGAGAGAACAGCGAGAATTCTG
MEG3-4 R	GTGCACAGATTTAGTTGAAGCCTG
IL1B F	GATGAATTGGTCATAGCCCGCAC
IL1B R	GTTTGTTTTAATGAAATTTATTTC
miR-138	AGCTGGTGTTGTGAATAGGCCG
GAPDH F	ACAACTTTGGCATTGTGGAA
GAPDH R	GATGCAGGGATGATGTTCTG
miR-302b	ACTTTAACATGGGAATGCTTTCT
IRAK4 F	ACTTCTCGAGAACCTGGAGACCGG
IRAK4 R	GTGCCAACTCGTCTATTAACTAAC
miR-138 pro	DIG-cagcugguguugugaaucaggccgacgagcagcgcauccucuuacccggcuauuucacgacaccaggguug
miR-302b pro	DIG-guucccuucaacuuuaacaugggaaugcuuucugucucaucgaagaguaagugcuuccauguuuuaguagaagu
For human macrophages	

MEG3-18 F	GCACTCCGCTTTGCTCTGTC
MEG3-18 R	CAGAGGGCTGTGGAGCTGAG
IL1B F	GCGAGGGAGAAACTGGCAGA
IL1B R	GCCATGGCTGCTTCAGACAC
miR-330-5p	TCTCTGGGCCTGTGTCTTAGGC
GAPDH F	CGGGAAACTGTGGCGTGATG
GAPDH R	ATGACCTTGCCCACAGCCTT